Journal of the Optical Society of Korea, Vol. 1, No. 2, September 1997, pp. 90-93

Microscopic Images with Extended Depth of Focus - Implementation and its Limitations

Kie B. Nahm, Eun S. Shin, and Seok M. Ryoo

Dept of Physics and Interdisciplinary Research Center Hallym University, Chunchon, Kangwon , 200-702, KOREA

(Received: August 1, 1997)

The shallow depth of focus in conventional light microscopy hinders the observation of the whole image when the object is thicker than the depth of field. Most of the existing techniques measured the object distance, which is not necessarily the actual distance of each pixel in the image. We implemented a means of determining the "best focus" of each pixel and located the height of object points by sectioning at different sample heights. Combining the height information and its gray values together, we obtained an image where the blur from the finite depth of focus is eliminated. Limitations of the technique are discussed together with composed images.

I. INTRODUCTION

An imaging system has many limitations in forming an image. Aberration is the primary element that degrades the image sharpness. Even with an aberration-free system, diffraction, an effect caused by the finite size of the aperture, sets the eventual limit of the spatial resolution. The depth of field (DOF) is another characteristic not associated with deficiencies of the system that still hinders the observer, especially in high power microscopy. DOF is a result of the image forming relations: the very relations relating the object-lens-image locations dictate that any object not on the location meeting the relations are imaged off focus. The amount of deviation which qualifies as out-of-focus is a very subjective matter. There is no analytic criteria to define the DOF : It is a quantity loosely defined for the conventional microscope as[1]

$$DOF \approx 2\,\frac{0.55}{(NA)^2}. \qquad (1)$$

where NA is the numerical aperture of the objective lens. According to (1), the DOF for 40× objective(NA 0.65) is 2.6μm, thereby making it difficult to observe specimens deeper than this value. When one observes such a specimen, it is necessary to move the sample up and down to bring different portions of the object into focus. Photographing the whole span of the sample depth in one frame is technically unrealistic in this case. In this article, we report a technique and an experimental arrangement that produces an image with an extended depth of focus using a conventional optical microscopic system. A frame grabber, connected to a PC, is the only extra hardware required to complete the system.

II. FOCUS DETECTION

The autofocus technique is readily available, and is widely used in cameras these days. There are a few different means of detecting the focus of an image in an automatic way. Most auto-focus cameras adopt active ranging techniques, using either time-of-flight (echo) or triangulation. Some more advanced models employ a passive detection scheme, utilizing a contrast measurement. This method is based on the property that the image has the sharpest lines when in focus. All of the above-mentioned techniques have one thing in common: they measure the representative focusing parameter for an over-all picture, not for every picture element in the frame. As such, unless the DOF is deep enough, some portions of the picture are bound to be out of focus. For this reason, autofocusing techniques, including the one based on astigmatic foci, are not applicable to microscope images when the height range of the specimen exceeds the DOF of the optical system.

The focused pixel does not always have the highest energy flux and intensity information is not adequate for use as a focus criteria. The gray value of a pixel is the result of the convolution of the system PSF and the object; it is affected, in principle, by all the pixel points in the plane preceeding the measuring one. We may reduce the influencing pixels to the nearest neighbors,but this still requires considerable amount of "deconvolution". The graph(a) in Fig. 1 shows the variation of the intensity of a pixel with defocus. The focused and averaged grey value was around 225. The point of best focus, denoted by the vertical line, displays no characteristic feature. The focal plane however guarantees that edges are sharpest and lines crispest, which is what made passive focus detection possible. As a

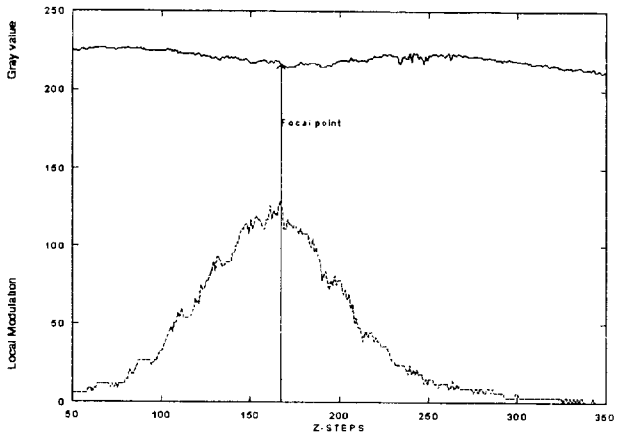

FIG. 1. Behavior of the pixel (a:top) and the modulation values (b: bottom), defined as per the relation (2), near the "focus height".

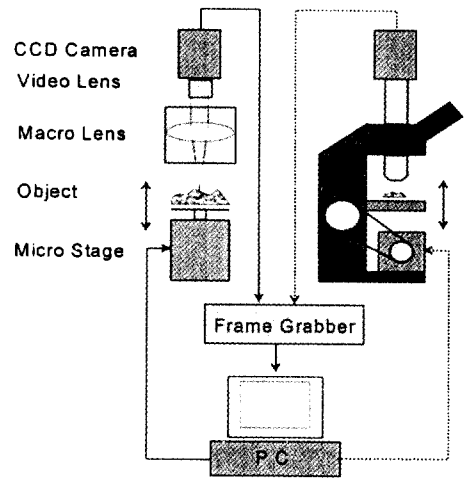

FIG. 2. The arrangement for the demonstration of extended depth of focus.

figure of merit for this characteristic on each pixel, we defined a quantity defined as follows.

$$\text{Focused Image}: f(x,y,z) = \frac{\sum_{i=-n}^{+n}\sum_{j=-n}^{+n}\{I(x+i,y+j,z)-I_m(x,y,z)\}^2}{I_m^2(x,y,z)} \quad (2)$$

$$\text{Averaged Intensity}: I_m(x,y,z) = \frac{1}{(2n+1)^2}\sum_{i=-n}^{n}\sum_{j=-n}^{n} I(x+i,y+j,z) \quad (3)$$

Here, the summation is over the neighboring (2n+1) × (2n+1) array of pixels, and the choice of n is decided by the quality of the image. The typical value of n is 2 or 3. The functional value represented by Eq.(2) is a measure of variation of the neighboring pixels around the local mean and the graph (b) in Fig. 1 is the experimental result of Eq.(2) for a spot on a reference image with varying z for a chosen pair of x and y, where the actual functional value was tripled for aesthetic reasons. The obvious peak, which we associate with the focal plane, is plainly observed. The z value corresponding to the peak of this curve is defined as the "focus height" of the image.

III. IMAGE WITH THE EXTENDED DEPTH OF FOCUS

The idea of locating the "focus height" defined in Eq.(2) is easily extended to the whole image. Once the image is captured and stored in the working memory of the computer, this procedure is applied to all the pixels in the target area. The result of Eq.(2) is stored for each pixel and the procedure is repeated for the next image slice. If the f value for the new slice is higher than the previous one, the location of the "focal height" is updated with the new z coordinate and the corresponding pixel data is stored separately. At the end of a run, one has all the information about image values, color and intensity, for all the pixels and "focus heights" of each pixel, stored in the memory. Neglecting the height and combining all the "focus" pixels produces an image with the extended depth of focus. To implement this idea, we installed a macro zoom lens directly in front of a standard 16mm CCD camera lens. The image from the camera was fed to a frame grabber, as shown in Fig. 2. A similar setup was installed on a conventional light microscope, where the CCD camera was fitted onto the conventional camera port(right side of Fig. 2, in dotted line). In both setups, the sample position along the z-axis could be controlled via the PC to within 2.5 μm. The two systems differed in optical arrangement; the microscope produced the true telecentric image.

Fig. 3 is the demonstration of this technique at work. Figs. 3-a) through 3-h) are the conventional close-up images with a shallow depth of field. As the sample is brought in, the region of exact focus spreads out, as should be expected from a convex object. Fig. 4

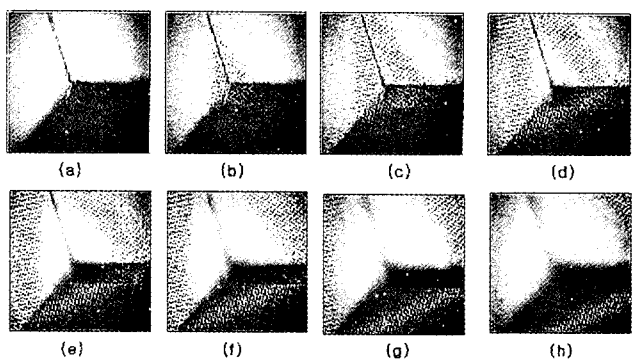

FIG. 3. Depth of field illustrated. As the sample moves in, the area of well defined foci moves out for a convex object.

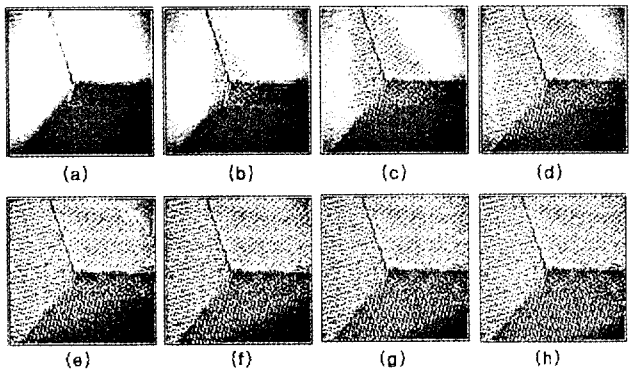

FIG. 4. The reconstruction of the image with the extended depth of field. As the slice is added up, the final image emerges in (h).

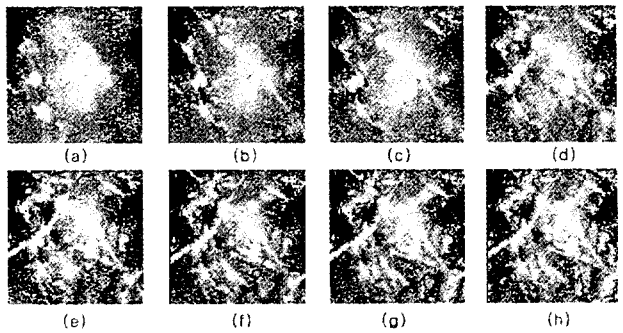

FIG. 5. Reconstruction of the fiber images from cleaning paper.

shows a series of images, composed of pixels that were determined to represent the best focus on each pixel, as the sample was brought in. Fig. 4-h) is the resultant image and the effect of the extended depth of focus is very noticeable. In this experiment, the object was a corner of a cube, whose outer walls were covered with minute patterns. These patterns were intentionally applied; the wall was flat in color and shade, which renders relation (2) useless in locating the peak. Fig. 5 shows the application of the same principle for the microscopic images. The sample was the edge of a torn paper observed with a 10× objective. The effect of the finite depth of focus as shown in Figs. 5-a) through g) is eliminated in the processed image with the extended focal depth, Fig. 5-h).

IV. LIMITS OF APPLICABILITY

IV. A. Flat object

The technique discussed so far relies on the variation of the gray tone around the point of interest. A flat object, which in this article is defined as one with slowly varying gray levels like the image of a white wall, does not display meaningful variations of the gray level, thus

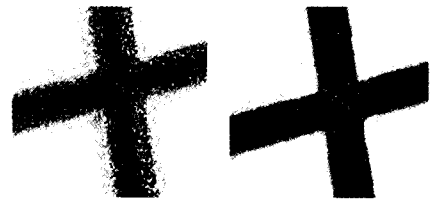

FIG. 6. Anormalies associated with flat objects. The composed image(left) is noisier than the best focus image. The object was a "+" on a tilted plane.

posing a serious technical challenge. Also included in this category are the images composed of flat patches, like the enlarged image of printed letters. Appropriate "height" information can not be retrieved within each patch, while the edge would be recovered successfully since there exists a rather rapid change in pixel values. The resulting image shows edges, with thickness corresponding to the size of the neighboring pixels used in the computation, and the areas inside the patches; the "height" of the pixel inside of the patches are not determined by the above-mentioned technique, and neither are the pixel values used to compose the final image. Fig. 6 is a demonstration of this phenomenon. One may overcome the problem by projecting a fine pattern onto the sample with an additional set-up and using the projected pattern as the guide to locating the "height". The spacing between the pattern should be such that, when imaged on the CCD, its size is smaller than the number of pixels used in the algorithm, typically 5 or 7. Since the physical dimension of the CCD pixel was close to 13μm , the projected spacing should, if a 7 x 7 processing array were to be used, be less than 13 x 7 x M (μm), where M is the magnification of the optical system. The result shown in Fig. 3 was obtained in this way , where in this case patterns were printed on a paper, which was wrapped around an object made of clear acrylic material. The detail of this application calls for further investigation.

IV. B. Discontinuity in the object

A deep cleavage or a narrow hole presents another kind of challenge. For the best result, we should expect to have the lowest possible depth of focus. Eq.(2) dictates that NA be as high as possible. This means a larger cone angle at the specimen. Thus, this system would function properly for a cone-shaped surface where the cone beam can reach as shown in Fig. 7. Any surface structure narrower than this configuration will block portions of the light scattered from the inner surface from reaching the focal plane on focus. A deep hole or a crevice also hinders the illuminating light from reaching deep inside. When the illumination comes from the top, as in the case of a reflection mode microscope, a great portion of the light converging to

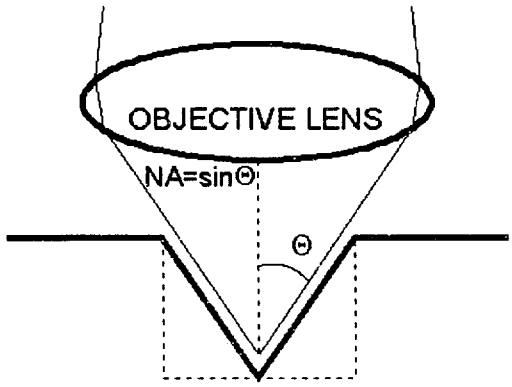

FIG. 7. Maximum detectable cone configuration. Any hole narrower than this can not be measured reliably.

the inside corner of a square hole, shown by dotted line in Fig. 6, would be blocked off. As a result of these combined effects, the image of a concave object narrower than the NA of the system would be noisier and its composed image quality would be degraded. Also the finite size of the focal point caused by diffraction will eventually deteriorate the spatial resolution in the horizontal direction.

V. CONCLUSIONS

It was discussed and demonstrated that defining the image sharpness of a pixel in the digitized image plane solely based on the gray value without referencing neighbors is unrealizable. Deconvolution is one approach to remove blur from the image and is a subject of serious investigation. It is not a straightforward application of mathematical relations. The phase information for the proper deconvolution is not available in all the conventional images and the deconvolved image thus obtained is not guaranteed to be the solid representation of the actual object. One can find extensive reviews in the related works by Shaw[3]and Holms[4]. The focus was reliably detected if the regional modulation was used as the indicator: the z coordinate that yielded the highest modulation to the mean gray value ratio should be the focal position. The minimum number of pixels for calculating the modulation was found to be 25 in a 5 x 5 array in the neighborhood of the pixel under study. A 7 x 7 array generates an image with a slightly improved quality at the expense of twice the previous processing time, yet the image from a 5 x 5 array was found adequate. This routine is applicable to objects whose surface height variation is not too abrupt. Any crevice to be imaged should have a geometrical shape wider than the probing beam, which is represented by the numerical aperture, NA. A flat object still defies proper analysis as per this technique and calls for an auxiliary setup to project fine patterns. This subject should be followed up in subsequent studies.

ACKNOWLEDGMENTS

This paper was supported by NON DIRECTED RESEARCH FUND, Korea Research Foundation, 1996.

REFERENCES

[1] Tympel, V., Proc. SPIE, **2984**, 190 (1997).
[2] Goldberg, N., "Camera Technology", (Academic Press 1992) Chapter 1.
[3] Shaw, P.J., Comparison of Wide-Field/Deconvolution and Confocal Microscopy for 3D Imaging, in "Handbook of Biological Confocal Microscopy", J. Pawley ed., (Plenum, New York, 1995) Chapter 23.
[4] Holmes T.J. et al, Light Microscopic Images Reconstructed by Maximum Likelyhood Deconvolution, in "Handbook of Biological Confocal Microscopy", J. Pawley ed., (Plenum, New York, 1995) Chapter 24.